Electronic Supplementary Material (ESI) for Physical Chemistry Chemical Physics.
This journal is © the Owner Societies 2024

Conformational equilibria in acrolein-CO_2: The crucial contribution of n → π* interactions unveiled by rotational spectroscopy

Hao Wang, [ab] Junhua Chen,[c] Xiao Tian, [a] Chenxu Wang, [a] Junlin Lan, [a] Xingchen Liu, [b] Zhenhua Zhang, [b] Xiaodong Wen, [b] and Qian Gou*[a]

[a] School of Chemistry and Chemical Engineering, Chongqing University, Daxuecheng South Rd. 55, 401331, Chongqing, China.

[b] State Key Laboratory of Coal Conversion, Institute of Coal Chemistry, Chinese Academy of Sciences, Taoyuan South Rd. 27, Taiyuan 030001, Shanxi, China.

[c] School of Pharmacy, Guizhou Medical University, Guiyang 550000, Guizhou, China.

* E-mail: qian.gou@cqu.edu.cn

Table of Contents

1. Shapes and principal inertial axes of six isomers of ACR-CO_2.

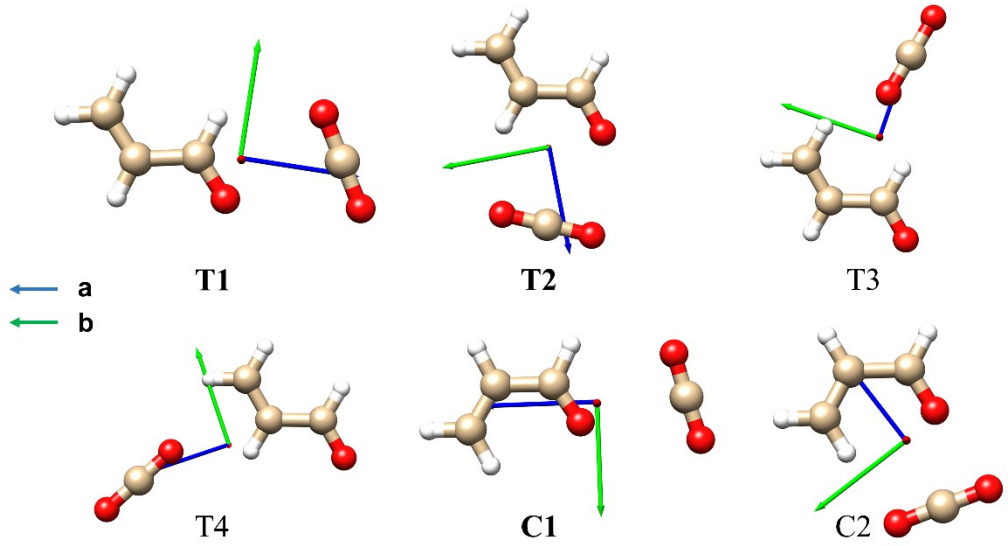

Fig. S1 Six isomers of ACR-CO_2 with the principal inertial axes at the B2PLYP-D3(BJ)/ 6-311++G(d,p) level of theory.

2. Molecular structures and the NCI isosurfaces for the six plausible isomers of ACR–CO_2.

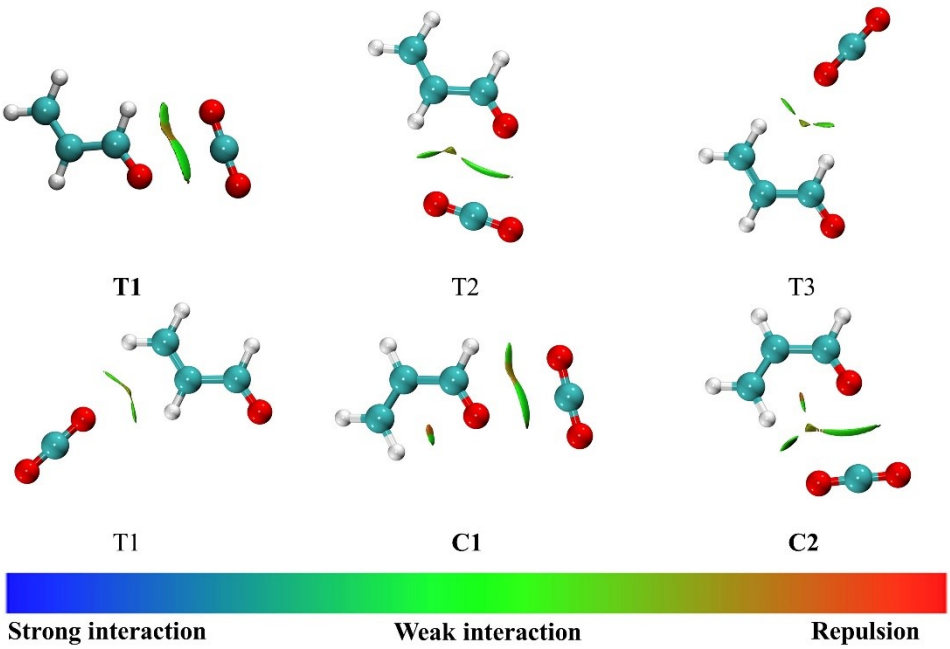

Fig. S2 Molecular structures and the NCI isosurfaces for the six plausible isomers of ACR–CO_2 predicted at the B2PLYP-D3(BJ)/6-311++G(d,p) level of theory. The NCI analyses based on the calculated structures, the gradient isosurfaces (s = 0.5 a.u.) are coloured on a blue-green-red scale scaling to values of the electron density.

3. Potential energy surface

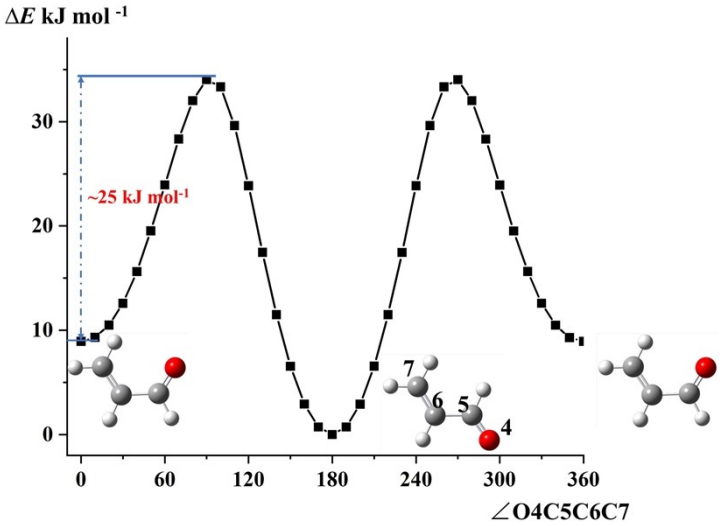

Fig. S3a The potential energy surface of cis/trans-ACR calculated at the B2PLYP-D3(BJ)/6-311++G(d,p) level of theory by changing the dihedral angle ∠O4C5C6C7. The E_{min} is -502992.8513 kJ mol^{-1}, and the E_{max} is -502958.8253 kJ mol^{-1}.

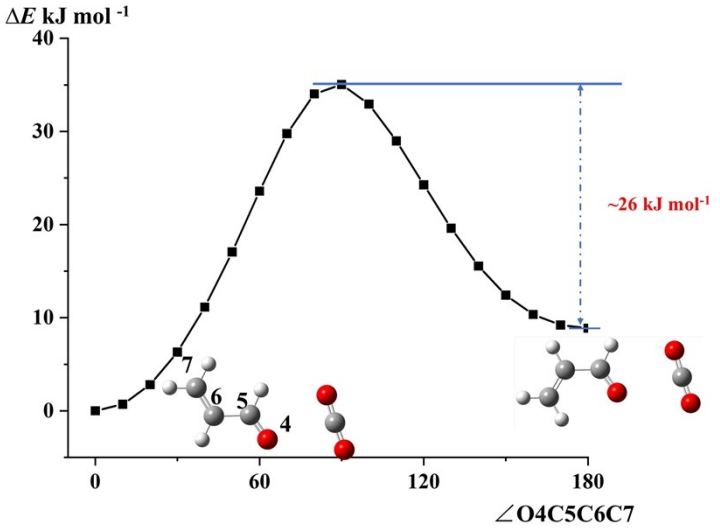

Fig. S3b The potential energy surface of **T1** to **C1** calculated at the B2PLYP-D3(BJ)/6-311++G(d,p) level of theory by changing the dihedral angle ∠O4C5C6C7. The E_{min} is -91970.43416 kJ mol^{-1}, and the E_{max} is -998469.6821 kJ mol^{-1}.

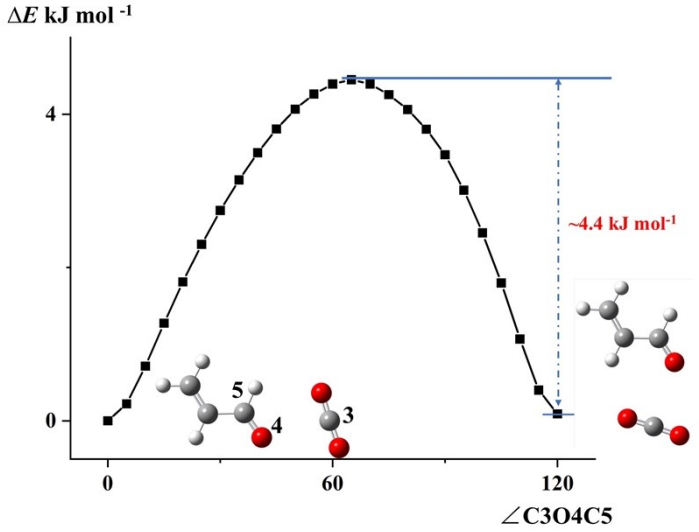

Fig. S3c The potential energy surface of **T1** to **T2** calculated at the B2PLYP-D3(BJ)/6-311++G(d,p) level of theory by changing the angle ∠C3O4C5. The E_{min} is -998469.6821 kJ mol^{-1}, and the E_{max} is -998465.2327 kJ mol^{-1}.

4. Intensities (in arbitrary units) of the three isomers for several μ_a-/μ_b- types selected

Table S1a Intensities (in arbitrary units) of **T1**/**T2** for several μ_a-/μ_b-type selected transitions.

Transitions	Isomer	Frequencies	Intensities
$3_{0\,3} \leftarrow 2_{0\,2}$	T1	5413.9034	0.3807
	T2	6302.9449	0.1804
$4_{0\,4} \leftarrow 3_{0\,3}$	T1	7213.6541	0.4920
	T2	8376.8283	0.1388
$6_{0\,6} \leftarrow 5_{0\,5}$	T1	10799.6403	0.0516
	T2	12453.2642	0.0274
$8_{0\,8} \leftarrow 7_{0\,7}$	T1	14361.1925	0.0148
	T2	16418.0371	0.0026
$1_{1\,1} \leftarrow 0_{0\,0}$	T1	8944.8338	0.1251
	T2	6675.4677	0.0489
$2_{1\,2} \leftarrow 1_{0\,1}$	T1	10651.2430	0.0887
	T2	8593.6244	0.0495
$3_{1\,3} \leftarrow 2_{0\,2}$	T1	12308.2173	0.0858
	T2	10418.6870	0.0265

Table S1b Intensities (in arbitrary units) of **T1**/**C1** for several μ_a-/μ_b-type selected transitions.

Transitions	Isomer	Frequencies	Intensities
$3_{0\,3} \leftarrow 2_{0\,2}$	T1	5413.9034	0.3807
	C1	5595.7700	0.0096
$4_{0\,4} \leftarrow 3_{0\,3}$	T1	7213.6541	0.4920
	C1	7455.3266	0.0149
$8_{0\,8} \leftarrow 7_{0\,7}$	T1	14361.1925	0.0148
	C1	14833.6573	0.0009
$1_{1\,1} \leftarrow 0_{0\,0}$	T1	8944.8338	0.1251
	C1	8898.7392	0.0034
$2_{1\,2} \leftarrow 1_{0\,1}$	T1	10651.2430	0.0887
	C1	10658.6485	0.0037
$3_{1\,3} \leftarrow 2_{0\,2}$	T1	12308.2173	0.0858
	C1	12365.5056	0.0041

5. Partial r_0 and B2PLYP-D3(BJ)/6-311++G(d,p) calculated geometries of ACR-CO_2 complexes

Table S2a Partial r_0 and B2PLYP-D3(BJ)/6-311++G(d,p) calculated geometries for **T1**.

Bond lengths (Å)		Valence angles (°)		Dihedral angles (°)	
O1O2	2.330				
O1C3	1.167	O2O1C3	1.2		
C3O4	**2.832(1)[a]**	**O1C3O4**	**87.1(3)**	O1C3O4O2	-180.0
O4C5	1.217	C3O4C5	111.4	C3O4C5O1	-0.0
C5C6	1.471	O4C5C6	124.0	O4C5C6C3	180.0
C6C7	1.339	C5C6C7	120.5	C5C6C7O4	-180.0
C6H8	1.084	C5C6H8	117.0	H8C6C5O4	0.0
C7H9	1.082	C6C7H9	122.1	H9C7C6C5	180.0
C7H10	1.085	C6C7H10	120.8	H10C7C6C5	-0.0
C5H11	1.107	C6C5H11	115.4	H11C5C6C7	-0.0

[a] Error in parentheses in units of the last digit. The parameters in bold have been adjusted to reproduce the experimental values of rotational constants. Their theoretical values are 2.821 Å and 87.3°, respectively.

Table S2b Partial r_0 and B2PLYP-D3(BJ)/6-311++G(d,p) calculated geometries for **T2**.

Bond lengths (Å)		Valence angles (°)		Dihedral angles (°)	
O1O2	2.329				
O2C3	1.167	O2O1C3	1.0		
C3O4	**2.892(2)[a]**	**O1C3O4**	**89.7(6)**	O2O1C3O4	180.0
O4C5	1.216	C3O4C5	128.9	O1C3O4C5	-0.0
C5C6	1.472	O4C5C6	124.4	C3O4C5C6	0.0
C6C7	1.339	C5C6C7	120.3	O4C5C6C7	180.0
C6H8	1.083	C5C6H8	117.0	O4C5C6O8	-0.0
C7H9	1.083	C6C7H9	122.0	C5C6C7H9	-180.0
C7H10	1.086	C6C7H10	120.9	C5 C6 C7H10	-0.0
C5H11	1.109	O4C5H11	120.6	C3O4C5H11	-180.0

[a] Error in parentheses in units of the last digit. The parameters in bold have been adjusted to reproduce the experimental values of rotational constants. Their theoretical values are 2.870 Å and 91.4°, respectively.

Table S2c Partial r_0 and B2PLYP-D3(BJ)/6-311++G(d,p) calculated geometries for **C1**.

Bond lengths (Å)		Valence angles (°)		Dihedral angles (°)	
O1O2	2.330				
O1C3	1.167	O2O1C3	1.2		
C3O4	**2.832(1)[a]**	**O1C3O4**	**87.3(9)**	O4C3O1O2	180.0
O4C5	1.217	C3O4C5	112.1	C5O4C3O1	-0.0
C5C6	1.482	O4C5C6	124.2	O4C5C6C3	180.0
C6C7	1.338	C5C6C7	121.6	C5C6C7O4	0.0

C6H8	1.084	C5C6H8	120.1	H8C7C6C5	0.0
C7H9	1.082	C6C7H9	122.1	H9C7C6C5	-180.0
C6H10	1.085	C6C7H10	116.9	H10C6C5O4	-180.0
C5H11	1.107	C6C5H11	115.9	H11C5C6C7	-180.0

[a] Error in parentheses in units of the last digit. The parameters in bold have been adjusted to reproduce the experimental values of rotational constants. Their theoretical values are 2.817 Å and 87.6°, respectively.

Table S2d The B2PLYP-D3(BJ)/6-311++G(d,p) calculated geometries for C2.

Bond lengths (Å)		Valence angles (°)		Dihedral angles (°)	
O1O2	2.329				
O1C3	1.167	O2O1C3	0.9		
C3O4	2.883	O1C3O4	91.4	O4C3O1O2	-180.0
O4C5	1.217	C3O4C5	151.4	C5O4C3O1	0.0
C5C6	1.482	O4C5C6	124.8	O4C5C6C3	0.0
C6C7	1.339	C5C6C7	122.0	C5C6C7O4	-0.0
C7H8	1.084	C6C7H8	120.6	H8C7C6C5	0.0
C7H9	1.082	C6C7H9	121.3	H9C7C6C5	-180.0
C6H10	1.085	C5C6H10	116.7	H10C6C5O4	180.0
C5H11	1.106	C6C5H11	115.3	H11C5C6C7	180.0

Table S2e The B2PLYP-D3(BJ)/6-311++G(d,p) calculated geometries for CO_2.

Bond lengths (Å)		Valence angles (°)		Dihedral angles (°)	
C1O2	1.165				
C1XX3[a]	1.000	O2O1XX3	90.0		
C1O4	1.165	O4C1XX3	90.0	O4O1XX3O2	180.0

[a] XX is a dummy atom.

6. NBO analysis for ACR-CO_2 (all values in kJ mol^{-1}).

Table S3a NBO energies (> 0.21 kJ mol^{-1}) of the **T1** complex.

Donor NBO	Acceptor NBO	E (kJ mol^{-1})	Complexes
From ACR to CO_2			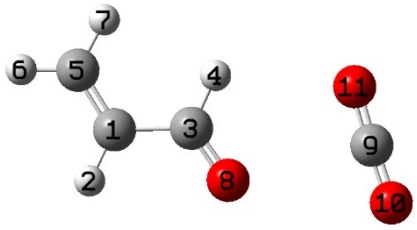
σ(1) C1 - C3	RY*(5) C9	0.33	
π(1) C3 – O8	RY*(1) C9	0.50	
π(1) C3 – O8	RY*(5) C9	0.25	
LP (1) O8	RY*(5) C9	0.54	
LP (1) O8	π*(3) C9 – O10	**1.97**	
LP (2) O8	RY*(6) C9	0.33	
LP (2) O8	π*(3) C9 – O10	**5.31**	
From CO_2 to ACR			
LP (1) O11	RY*(4) H4	0.46	
LP (1) O11	σ*(1) C3 – H4	**0.29**	
LP (2) O11	σ*(1) C3 – H4	**0.25**	

Table S3b NBO energies (> 0.21 kJ mol^{-1}) of the **T2** complex.

Donor NBO	Acceptor NBO	E (kJ mol^{-1})	Complexes
From ACR to CO_2			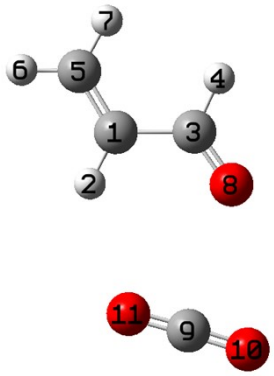
π(1) C3 – O8	RY*(1) C9	0.29	
π(1) C3 – O8	RY*(6) C9	0.46	
LP (1) O8	RY*(5) C9	0.33	
LP (1) O8	π*(3) C9 – O10	**2.17**	
LP (2) O8	π*(3) C9 – O10	**3.18**	
From CO_2 to ACR			
LP (1) O11	RY*(1) H2	0.92	
LP (1) O11	σ*(1) C1 – H2	**1.05**	
LP (2) O11	RY*(1) H2	0.42	
LP (2) O11	σ*(1) C1 – H2	**0.96**	

Table S3c NBO energies (> 0.21 kJ mol^{-1}) of the **T3** complex.

Donor NBO	Acceptor NBO	E (kJ mol^{-1})	Complexes
From ACR to CO_2			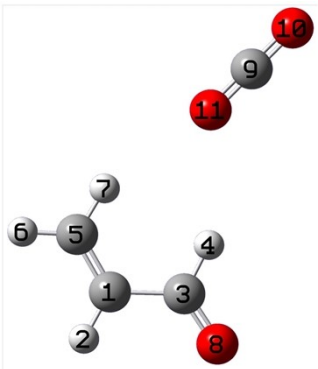
-	-	-	
From CO_2 to ACR			
π(1) C9 – O11	RY*(2) H4	0.29	
π(1) C9 – O11	RY*(1) H7	1.80	
LP (1) O11	RY*(3) H4	0.29	
LP (1) O11	RY*(1) H7	0.59	
LP (1) O11	σ*(1) C3 – H4	0.88	
LP (1) O11	σ*(1) C5 – H7	1.05	
LP (2) O11	σ*(1) C3 – H4	0.59	

Table S3d NBO energies (> 0.21 kJ mol^{-1}) of the **T2** complex.

Donor NBO	Acceptor NBO	E (kJ mol^{-1})	Complexes
From ACR to CO_2			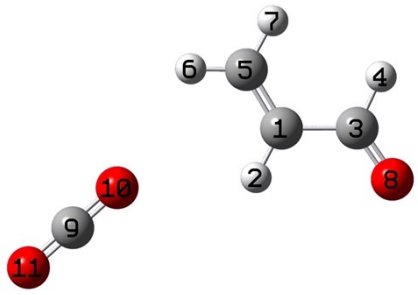
-	-	-	
From CO_2 to ACR			
π(1) C9 – O10	RY*(1) H6	0.79	
LP (1) O10	RY*(1) H2	0.33	
LP (1) O10	RY*(1) H6	0.38	
LP (1) O10	σ*(1) C1 – H2	0.29	
LP (1) O10	σ*(1) C5 – H6	0.46	
LP (3) O10	σ*(1) C1 – H2	0.42	

Table S3e NBO energies (> 0.21 kJ mol^{-1}) of the **C1** complex.

Donor NBO	Acceptor NBO	E (kJ mol^{-1})	Complexes
From ACR to CO_2			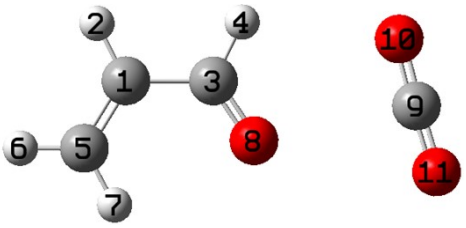
σ(1) C1 – C3	RY*(5) C9	0.29	
π(1) C3 – O8	RY*(1) C9	0.50	
π(1) C3 – O8	RY*(5) C9	0.29	
π(1) C3 – O8	RY*(3) O11	0.25	
LP (1) O8	RY*(5) C9	0.63	
LP (1) O8	RY*(3) O11	0.25	
LP (1) O8	π*(3) C9 – O11	**2.01**	
LP (2) O8	RY*(6) C9	0.33	
LP (2) O8	π*(3) C9 – O11	**5.56**	
From CO_2 to ACR			
π(1) C9 – O10	RY*(3) C3	0.33	
LP (1) O10	RY*(4) H4	0.46	
LP (1) O10	σ*(1) C1 – C3	0.25	
LP (2) O10	σ*(1) C3 – H4	**0.25**	

Table S3f NBO energies (> 0.21 kJ mol^{-1}) of the **C2** complex.

Donor NBO	Acceptor NBO	E (kJ mol^{-1})	Complexes
From ACR to CO_2			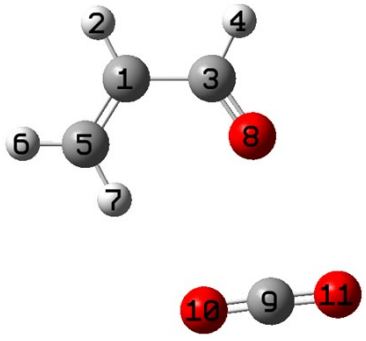
σ(1) C1 – H2	RY*(5) O10	0.33	
π(1) C3 – O8	RY*(4) C9	0.33	
π(1) C3 – O8	RY*(5) C9	0.75	
π(1) C3 – O8	RY*(3) O11	0.25	
π(2) C3 – O8	RY*(7) C9	0.25	
σ(1) C5 – H6	RY*(6) C9	0.21	
σ(1) C5 – H6	RY*(7) O10	0.21	
LP (1) O8	RY*(5) C9	0.29	
LP (1) O8	RY*(3) O11	0.29	
LP (1) O8	π*(3) C9 – O11	**2.72**	
LP (2) O8	π*(3) C9 – O11	**1.38**	
From CO_2 to ACR			
π(3) C9 – O11	π*(1) C3 – O8	0.33	
LP (1) O10	RY*(1) H7	0.71	
LP (1) O10	RY*(3) H7	0.21	

LP (1) O10	RY*(4) H7	0.21	
LP (1) O10	σ*(1) C5 – H7	**1.46**	
LP (2) O10	RY*(1) H7	0.67	
LP (2) O10	σ*(1) C5 – H7	**2.51**	
LP (1) O11	RY*(1) H7	0.33	
π(2) C9 – O11	π*(2) C3 – O8	0.25	
π(3) C9 – O11	RY*(1) H7	0.21	

7. Result of NAOs analysis

Table S4a NAO analysis for **T1** about TB binding orbital.

Index	Occupancies	Bond orbital	Natural population	Complexes
21	1.98	LP (1) O8	s 59.07%, p 40.77%	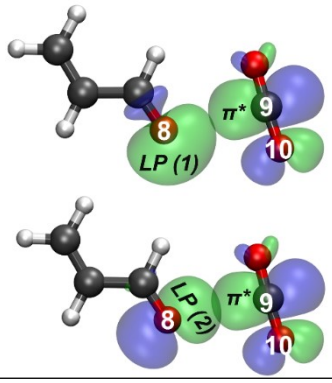
22	1.91	LP (2) O8	s 0.03%, p 99.74%	
413	0.31	π* (3) C9 = O10	C: s 0.39%, p 79.80% O: s 0.10%, p 19.33%	

Table S4b NAO analysis for **T2** about TB binding orbital.

Index	Occupancies	Bond orbital	Natural population	Complexes
21	1.98	LP (1) O8	s 58.96%, p 40.89%	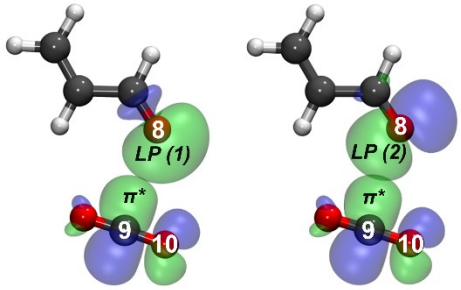
22	1.90	LP (2) O8	s 0%, p 99.76%	
413	0.30	π* (3) C9 = O10	C: s 0.51%, p 79.67% O: s 0.08%, p 19.36%	

Table S4c NAO analysis for **C1** about TB binding orbital.

Index	Occupancies	Bond orbital	Natural population	Complexes
21	1.98	LP (1) O8	s 59.06%, p 40.79%	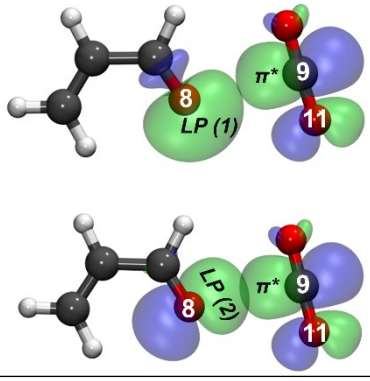
22	1.91	LP (2) O8	s 0.08%, p 99.69%	
414	0.31	π* (3) C9 = O11	C: s 0.36%, p 79.87% O: s 0.10%, p 19.30%	

Table S4d NAO analysis for **C2** about TB binding orbital.

Index	Occupancies	Bond orbital	Natural population	Complexes
21	1.98	LP (1) O8	s 58.81%, p 41.06%	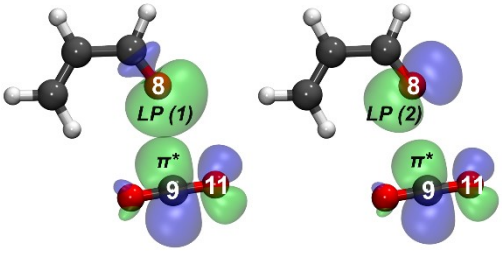
22	1.91	LP (2) O8	s 0.02%, p 99.73%	
414	0.31	π* (3) C9 = O11	C: s 0.43%, p 79.78% O: s 0.06%, p 19.35%	

8. NBO analysis for ACR-CO_2 about TB binding orbitals

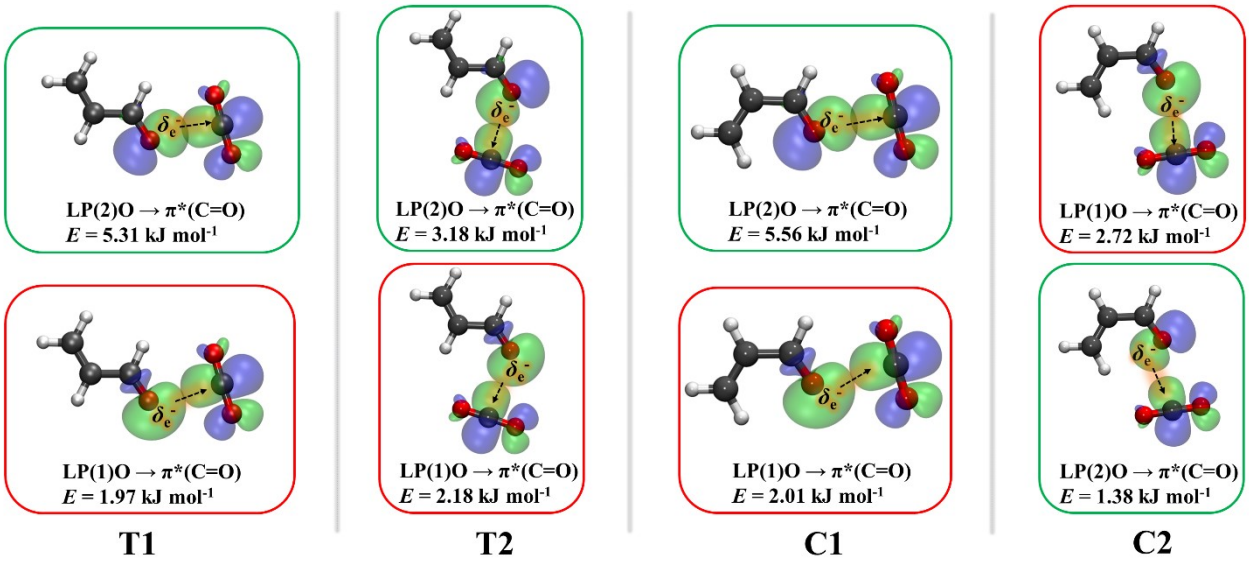

Fig. S4 The n → π* interactions of four ACR-CO_2 clusters by NBO analyses. Green frames: n_p → π*; red frames: n_s → π* (see Table S4).

9. Measured Transition Frequencies

Table S5 μ_a/μ_b-type transition frequencies (ν/MHz) and corresponding observed – calculated deviations ($\Delta\nu$/kHz) for **T1**.

Transitions		ν/MHz	$\Delta\nu$/kHz
J′ K_a′ K_c′ ←	J″ K_a″ K_c″		
3 0 3	2 0 2	5413.9034	0.2
3 1 3	2 1 2	5267.9892	0
3 1 2	2 1 1	5566.8336	0.2
3 2 2	2 2 1	5418.1045	1.7
3 2 1	2 2 0	5422.2425	0
4 0 4	3 0 3	7213.6541	0.4
4 1 4	3 1 3	7022.7427	0.4
4 1 3	3 1 2	7421.1545	0.1
4 2 3	3 2 2	7223.2729	-0.4
4 2 2	3 2 1	7233.6171	0
5 0 5	4 0 4	9009.2352	0.1
5 1 5	4 1 4	8776.4501	0.1
5 1 4	4 1 3	9274.3500	0.3
5 2 4	4 2 3	9027.7044	0.3
5 2 3	4 2 2	9048.3693	-0.1
5 3 3	4 3 2	9033.6100	-2.8
5 3 2	4 3 1	9033.7499	-4
6 0 6	5 0 5	10799.6403	-2.2
6 1 6	5 1 5	10528.8765	0.6
6 1 5	5 1 4	11126.1132	0.6
6 2 5	5 2 4	10831.2108	0.5
6 2 4	5 2 3	10867.3068	0.3
7 0 7	6 0 6	12583.9202	0.2
7 1 7	6 1 6	12279.8010	0.7
7 1 6	6 1 5	12976.1195	0
7 2 6	6 2 5	12633.6088	1
7 2 5	6 2 4	12691.1857	-0.3
8 0 8	7 0 7	14361.1925	0.9
8 1 8	7 1 7	14029.0234	1.1
8 1 7	7 1 6	14824.0262	-0.2
8 2 7	7 2 6	14434.7149	1.5
8 2 6	7 2 5	14520.6861	0.7
8 3 6	7 3 5	14459.1282	1.7
8 3 5	7 3 4	14460.8142	-2

9 0 9	8 0 8	16130.7009	-1.1
9 1 9	8 1 8	15776.3643	1.3
9 1 8	8 1 7	16669.4632	-1.9
9 2 8	8 2 7	16234.3458	1.1
9 2 7	8 2 6	16356.3624	2.6
10 0 10	9 0 9	17891.8612	-1.9
10 1 10	9 1 9	17521.6665	-0.6
1 1 0	1 0 1	7238.4227	-1.1
1 1 1	0 0 0	8944.8338	0
2 1 1	2 0 2	7339.0880	-0.6
2 1 2	1 0 1	10651.2430	0.2
3 1 2	3 0 3	7492.0186	-0.2
3 1 3	2 0 2	12308.2173	0.1
4 1 3	4 0 4	7699.5198	0.2
4 1 4	3 0 3	13917.0560	-0.2
5 1 4	5 0 5	7964.6341	-0.1
5 1 5	4 0 4	15479.8528	0.2
6 1 5	6 0 6	8291.1047	0.5
6 1 6	5 0 5	16999.4927	-0.6
7 1 6	7 0 7	8683.3027	-1
8 1 7	8 0 8	9146.1400	1.3
8 0 8	7 1 7	8465.4591	-1.4

Table S6. μ_a/μ_b-type transition frequencies (ν/MHz) and corresponding observed – calculated deviations ($\Delta\nu$/kHz) for **T2**.

Transitions		ν/MHz	$\Delta\nu$/kHz
J' K_a' K_c' ←	J'' K_a'' K_c''		
2 0 2	1 0 1	4211.7185	0
2 1 2	1 1 1	4026.9515	0.4
2 1 1	1 1 0	4408.2080	-0.1
3 0 3	2 0 2	6302.9449	0
3 1 3	2 1 2	6036.7803	-0.2
3 1 2	2 1 1	6608.5305	0.6
3 2 2	2 2 1	6326.3865	0.1
3 2 1	2 2 0	6349.7242	0.7
4 0 4	3 0 3	8376.8283	-0.2
4 1 4	3 1 3	8042.3905	-0.4
4 1 3	3 1 2	8804.1567	0.8
4 2 3	3 2 2	8430.5247	-0.2
4 2 2	3 2 1	8488.6225	-0.2
4 3 2	3 3 1	8446.5942	-0.8
4 3 1	3 3 0	8447.2676	1
5 0 5	4 0 4	10428.2612	-0.6
5 1 5	4 1 4	10042.6308	0
5 1 4	4 1 3	10993.2573	0.7
5 2 4	4 2 3	10530.6780	0.3
5 2 3	4 2 2	10645.8777	0.2
5 3 3	4 3 2	10562.7965	-1.2
5 3 2	4 3 1	10565.1426	-1.9
6 0 6	5 0 5	12453.2642	-1.2
6 1 6	5 1 5	12036.5578	2
6 1 5	5 1 4	13173.7739	0.6
6 2 5	5 2 4	12625.8614	1
6 2 4	5 2 3	12824.4341	2.1
6 3 4	5 3 3	12681.4453	-3
6 3 3	5 3 2	12687.6886	-2
7 0 7	6 0 6	14449.7286	-0.2
7 1 7	6 1 6	14023.4631	0.2
7 1 6	6 1 5	15343.3634	0.3
7 2 6	6 2 5	14715.1077	2.4
7 2 5	6 2 4	15025.3441	1.7
7 3 5	6 3 4	14802.4782	0.1

7 3 4	6 3 3	14816.4654	-0.3
8 0 8	7 0 7	16418.0371	-0.7
8 1 8	7 1 7	16002.9158	3.1
1 1 0	1 0 1	4757.3041	-3.1
1 1 1	0 0 0	6675.4677	0.5
2 1 1	2 0 2	4953.7958	-1.1
2 1 2	1 0 1	8593.6245	-0.3
3 1 2	3 0 3	5259.3802	-1.7
3 1 3	2 0 2	10418.6870	0
4 1 3	4 0 4	5686.7085	-0.8
4 1 4	3 0 3	12158.1318	-1.3
5 1 4	5 0 5	6251.7034	-0.6
5 0 5	4 1 4	6646.9580	0.7
5 1 5	4 0 4	13823.9368	1.3
6 1 5	6 0 6	6972.2145	2.6
6 0 6	5 1 5	9057.5919	0
6 1 6	5 0 5	15432.2281	-1.2
7 1 6	7 0 7	7865.8468	0.7
7 0 7	6 1 6	11470.7633	-1.6
7 1 7	6 0 6	17002.4281	1.3
8 0 8	7 1 7	13865.3358	-4.2

Table S7. μ_a/μ_b-type transition frequencies (ν/MHz) and corresponding observed – calculated deviations ($\Delta\nu$/kHz) for the **C1**.

Transitions		ν/MHz	$\Delta\nu$/kHz
J' K_a' K_c' ←	J'' K_a'' K_c''		
3 0 3	2 0 2	5595.7700	-0.1
3 1 3	2 1 2	5439.4111	0.5
3 1 2	2 1 1	5760.2868	0
4 0 4	3 0 3	7455.3266	0
4 1 4	3 1 3	7251.1029	-1
4 1 3	3 1 2	7678.8852	0
5 0 5	4 0 4	9310.0215	1.1
5 1 5	4 1 4	9061.5854	-0.3
5 1 4	4 1 3	9596.1741	-0.6
6 0 6	5 0 5	11158.6884	1.4
6 1 6	5 1 5	10870.5849	0
6 1 5	5 1 4	11511.7946	-1.2
7 0 7	6 0 6	13000.2281	-0.4
7 1 7	6 1 6	12677.8510	0
7 1 6	6 1 5	13425.3675	0.2
8 0 8	7 0 7	14833.6573	0
8 1 8	7 1 7	14483.1580	0.1
8 1 7	7 1 6	15336.4812	-0.1
1 1 0	1 0 1	7138.8178	-0.6
1 1 1	0 0 0	8898.7392	-1.2
2 1 1	2 0 2	7246.9876	-0.9
2 1 2	1 0 1	10658.6485	1.9
3 1 2	3 0 3	7411.5056	0.4
3 1 3	2 0 2	12365.5056	0
4 1 3	4 0 4	7635.0648	0.9
4 1 4	3 0 3	14020.8389	-0.5
5 1 4	5 0 5	7921.2188	0.5
5 1 5	4 0 4	15627.0986	0
6 1 5	6 0 6	8274.3248	-2.3
6 1 6	5 0 5	17187.6632	0.1
7 1 6	7 0 7	8699.4674	1.5